The EMBO Journal (2012) 31, 1080–1094 | © 2012 European Molecular Biology Organization | All Rights Reserved 0261-4189/12
www.embojournal.org

THE EMBO JOURNAL

Oxidative stress induces an ATM-independent senescence pathway through p38 MAPK-mediated lamin B1 accumulation

Aurelia Barascu[1,2], Catherine Le Chalony[1,2], Gaëlle Pennarun[1,2], Diane Genet[1,2], Naima Imam[1,2], Bernard Lopez[1,2,*] and Pascale Bertrand[1,2,*]

[1]CNRS, UMR217, Fontenay aux Roses, France and [2]CEA, DSV, Institut de Radiobiologie Cellulaire et Moléculaire, Fontenay aux Roses, France

We report crosstalk between three senescence-inducing conditions, DNA damage response (DDR) defects, oxidative stress (OS) and nuclear shape alterations. The recessive autosomal genetic disorder Ataxia telangiectasia (A-T) is associated with DDR defects, endogenous OS and premature ageing. Here, we find frequent nuclear shape alterations in A-T cells, as well as accumulation of the key nuclear architecture component lamin B1. Lamin B1 overexpression is sufficient to induce nuclear shape alterations and senescence in wild-type cells, and normalizing lamin B1 levels in A-T cells reciprocally reduces both nuclear shape alterations and senescence. We further show that OS increases lamin B1 levels through p38 Mitogen Activated Protein kinase activation. Lamin B1 accumulation and nuclear shape alterations also occur during stress-induced senescence and oncogene-induced senescence (OIS), two canonical senescence situations. These data reveal lamin B1 as a general molecular mediator that controls OS-induced senescence, independent of established Ataxia Telangiectasia Mutated (ATM) roles in OIS.

The EMBO Journal (2012) **31,** 1080–1094. doi:10.1038/emboj.2011.492; Published online 13 January 2012
Subject Categories: genome stability & dynamics; molecular biology of disease
Keywords: Ataxia telangiectasia; lamin B1; oxidative stress; p38 MAPK; senescence

Introduction

Senescence is an essential process that should be tightly controlled. Indeed, on the one hand, senescence prevents the proliferation of cells bearing damaged DNA, constituting thus a barrier against tumour development. Consistently, senescence can be induced by replicative stress or oncogene expression (Collado and Serrano, 2010). On the other hand, in contrast, beside its putative role in organism ageing, recent data have proposed that senescent cells could favour tumour proliferation or invasion by secreting inflammatory factors (Rodier *et al*, 2009; Campisi *et al*, 2011; Rodier and Campisi, 2011).

Since Harman proposed the free radical theory of ageing in 1956, oxidative stress (OS) remains one of the most common causes cited for ageing. However, the precise molecular control of senescence induced by OS is far from being fully elucidated (Muller *et al*, 2007; Gil Del Valle, 2010). In addition to OS, telomere erosion, defects in the DNA damage response (DDR) and alterations of the nuclear architecture are also associated with premature ageing (Lans and Hoeijmakers, 2006). However, the potential interplay between these different processes leading to senescence remains poorly understood, and no unifying model can be drawn.

Ataxia telangiectasia (A-T), an autosomal-recessive genetic disorder, represents a paradigm to analyse the relationships between these senescence processes because it is associated with DDR defects, high levels of endogenous OS and premature ageing (Lavin, 2008). The Ataxia Telangiectasia Mutated (*ATM*) gene encodes a protein kinase that regulates the early step(s) of DNA damage signalling and thereby controls DDR (Rotman and Shiloh, 1999; Shiloh, 2006; Bartek *et al*, 2007; Cann and Hicks, 2007; Lavin and Kozlov, 2007; Matsuoka *et al*, 2007; Lavin, 2008). Consequently, mutations in *ATM* account for the DDR defects leading to some of the clinical features of A-T, including radiation sensitivity, genetic instability, immunodeficiency and cancer predisposition. However, the clinical picture of A-T is more complex, and the relationships between DDR defects, neurological disorders and premature ageing remain elusive. Recent data show that ATM is an important sensor of reactive oxygen species (ROS) in human cells and controls OS response; therefore, ATM deficiency accounts for the increase of ROS in A-T cells (Guo *et al*, 2010; Cosentino *et al*, 2011). High levels of endogenous OS may be responsible for the senescence and neurological phenotypes seen in A-T (Barzilai *et al*, 2002; Browne *et al*, 2004; Lavin *et al*, 2007; Reliene and Schiestl, 2007; Reliene *et al*, 2008). However, the mechanisms by which OS causes senescence and neurological disorders in A-T are still uncharacterized.

ATM has been proposed to participate in senescence induced by diverse stimuli (e.g., oncogenes, hyper-replication and DNA damage) (Bartkova *et al*, 2006; Di Micco *et al*, 2006). However, in contrast, ATM has a limited role in oncogene-induced senescence (OIS) in mice (Efeyan *et al*, 2009). Moreover, the observation that A-T cells undergo accelerated ageing supports the existence of ATM-independent senescence pathways. The p38 Mitogen Activated Protein (MAP) kinase has been proposed to participate in this alternative pathway (Naka *et al*, 2004). p38 MAPK also participates in senescence caused by diverse stresses (e.g., OS or after an oncogenic signal), but the precise mechanisms by

*Corresponding authors. B Lopez or P Bertrand, CNRS, UMR217, 18 route du panorama, Fontenay aux Roses 92265, France and CEA, DSV, IRCM, 18 route du panorama, Fontenay aux Roses 92265, France.
Tel.: +33 146548835; Fax: +33 146548955;
E-mail: bernard.lopez@cea.fr or Tel.: +33 146548846;
Fax: +33 146548955; E-mail: pascale.bertrand@cea.fr

Received: 25 March 2011; accepted: 19 December 2011; published online: 13 January 2012

which it induces senescence is far from being fully characterized (Wang *et al*, 2002; Iwasa *et al*, 2003; Debacq-Chainiaux *et al*, 2010).

Progeroid syndromes have been classified into two categories: DDR defect syndromes (including A-T), and laminopathies in which lamin A is altered (Lans and Hoeijmakers, 2006). Lamins A/C, B1 and B2 are major constituents of the inner nuclear membrane and determine its shape and integrity (Goldman *et al*, 2002; Gruenbaum *et al*, 2005; Misteli and Scaffidi, 2005; Broers *et al*, 2006; Prokocimer *et al*, 2009; Dechat *et al*, 2010). Remarkably, the alteration of the nuclear shape is generally associated with senescence. Indeed, the most severe premature ageing syndromes, such as Hutchinson Gilford's syndrome or atypical Werner's syndrome, are associated with alterations of the nuclear shape resulting from the deregulation of lamin A/C (Kudlow *et al*, 2007; Worman and Bonne, 2007; Ding and Shen, 2008). More generally, changes in the nuclear architecture also appear during the ageing process of wild-type (WT) cells, showing the importance of such alterations in general senescence processes (Haithcock *et al*, 2005; Scaffidi and Misteli, 2006; Cao *et al*, 2007; McClintock *et al*, 2007; Li *et al*, 2009; Rodriguez *et al*, 2009).

During a comparative proteomics study (data to be published), we observed an upregulation of lamin B1 in A-T cell extracts. Because A-T patients suffer from premature ageing, this observation led to the hypothesis that lamin B1 dysregulation could account for senescence in A-T cells, thus acting as a key player in an ATM-alternative senescence pathway. Here, we analysed and documented the origin of lamin B1 upregulation in A-T cells and its consequences on nuclear architecture and senescence. More generally, our data shed light on a general pathway of senescence, independent of ATM, in response to OS, namely the alteration of nuclear architecture due to the accumulation of lamin B1 via p38 MAPK activation.

Results

Lamin B1 protein levels are increased in A-T cells

Western blot analysis showed that lamin B1 was increased between three-fold and five-fold in different A-T lymphoblast cell lines relative to WT cells (Figure 1A). Lamin B1 was also increased in A-T primary fibroblasts, as detected by different antibodies raised against lamin B1 (Figure 1B; Supplementary Figure S1), demonstrating that lamin B1 overexpression in A-T cells is independent of cell type. Imaging analysis that monitored the mean lamin B1 fluorescence intensity per nucleus confirmed the three-fold increase of lamin B1 level in A-T cells compared with WT cells (Supplementary Figure S2A). Finally, among lamins family, only lamin B1 was overexpressed in A-T cells. Indeed, lamin A, lamin C and lamin B2 were not increased in A-T fibroblast cell extracts.

Notably, the A-T cells used were derived from different patients and harboured different mutations in the *ATM* gene, suggesting that lamin B1 overexpression is not associated with one specific mutation of ATM but is rather a general phenomenon that results from ATM inactivation. Consistent with this conclusion, inactivation of ATM by a specific chemical inhibitor (KU-55933) also led to an increase in lamin B1 protein levels in WT cells (Figure 1C).

Nuclear architecture is altered in A-T primary fibroblasts

Because lamin B1 is an essential component of the inner nuclear membrane, we examined the consequences of high lamin B1 protein levels on nuclear shape.

Immunofluorescence microscopy analysis showed that in the absence of any exogenous challenge, A-T primary fibroblasts frequently exhibited nuclear malformations (Figure 2A). Typical examples of alterations, specifically budded or folded nuclei, are shown (Figure 2A, left panels). The nuclear circularity of WT and A-T cell populations was quantified by image analysis. The mean circularity was significantly lower in two A-T compared with two WT primary fibroblasts (Figure 2A, right panels). The mean circularity measured in both A-T primary fibroblasts was significantly lower than the value of 0.65, in contrast with the two WT fibroblasts. Interestingly, at this circularity value an alteration of the nuclear envelope was unambiguously observed (Figure 2, upper panels). Thus, the circularity value of 0.65 was used as the cutoff for nuclear deformation for all subsequent analyses. The frequency of deformed nuclei (circularity $\leqslant 0.65$) increased from 16.8 and 16.6% in WT cells (GM03348 and GM05757, respectively) to 57.5 and 48.1% in A-T cells (GM05823 and GM02052, respectively) (Figure 2A, right panels). Using the values of lamin B1 fluorescence intensity and the values of nuclei circularity, we can see that more the intensity of lamin B1 increases more the value of circularity decreases (Supplementary Figure S2B).

To address whether the misshapen nuclei of A-T cells resulted from lamin B1 accumulation, we overexpressed lamin B1 in WT primary fibroblasts and monitored the nuclear shape by immunofluorescence (Figure 2B). The frequency of cells with mishappen nuclei (nucleus circularity $\leqslant 0.65$) was 62.3% in cells transfected with a lamin B1 expression vector compared with 16.1% in cells transfected with an empty expression vector (Figure 2B). Thus, the overexpression of lamin B1 alone was sufficient to induce nuclear deformation in WT fibroblasts to a similar extent as in A-T primary fibroblasts.

Lamin B1 overexpression induces senescence in primary fibroblasts

Because nuclear alteration is associated with senescence, we examined the consequences of lamin B1 overexpression on senescence in human primary fibroblasts.

Senescence is characterized by a loss of proliferation, an increase in senescence-associated β-galactosidase (SA-β-gal) activity and an alteration in chromatin structure. We first confirmed the senescent phenotype of A-T cells using SA-β-gal assay (Figure 3A). The percentage of SA-β-gal-positive cells in A-T population increased as early as passage 12 and reached 73% at passage 22, whereas only 15% of the WT population was senescent.

Interestingly, overexpression of lamin B1 in WT primary fibroblasts increased the frequency of SA-β-gal-positive cells from 16% in cells transfected with an empty expression vector to 60% in lamin B1-transfected cells (Figure 3B).

We also observed that lamin B1 overexpression resulted in an 'aggregation-compaction' of 4′-6-diamidino-2-phenylindole (DAPI) staining (Figures 2B and 3C, yellow arrows), which is indicative of senescence-associated heterochromatin foci (SAHF). To confirm these interpretations, we examined

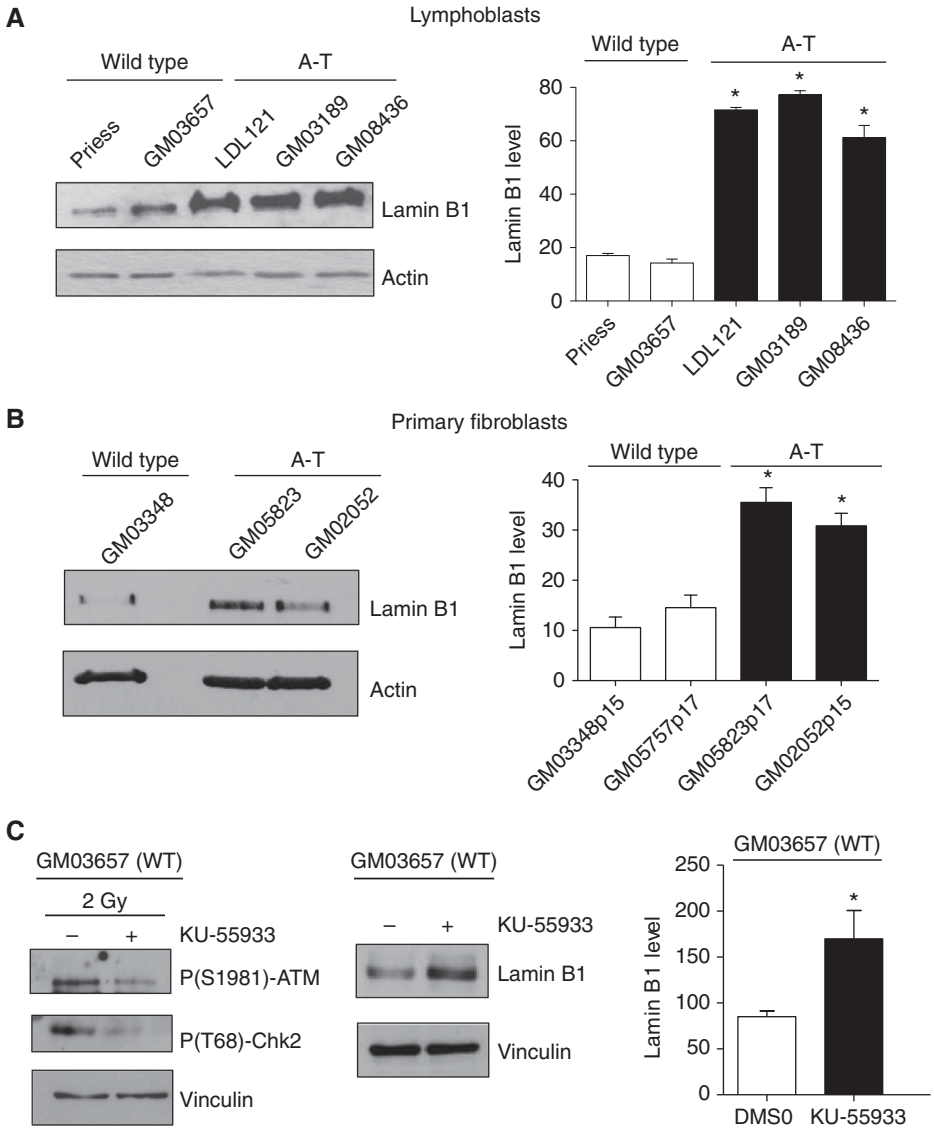

Figure 1 Increase of lamin B1 levels in A-T cells. Western blot analysis of extracts (**A**) from wild-type (WT) and A-T lymphoblasts and (**B**) from WT (GM03348 p15) and A-T primary fibroblasts (GM05823 p17 and GM02052 p15). Right panels: quantification of lamin B1 levels relative to actin. (**C**) Increase of lamin B1 after ATM inhibition. WT lymphoblasts were treated for 24 h with DMSO or 10 μM KU-55933, a specific ATM inhibitor. Left panel: control of inhibitor efficiency by western blot analysis of ATM activity using the ATM-P(S1981) and Chk2-P(T68) antibodies, after irradiation at 2 Gy. Right panel: the western blot analysis and quantification (histogram) show an increase of lamin B1 levels in WT lymphoblasts (GM03657) after 24 h of KU-55933 treatment. All quantification values correspond to at least three independent experiments. *Represents a statistically significant difference ($P<0.05$) between the values for WT and A-T cells or between untreated and treated cells. The error bars denote the s.e.m.

the expression of heterochromatin protein 1 (HP1) and histone H3 dimethylated on lysine 9 (H3mK9) by immunofluorescence. Overexpression of lamin B1 efficiently induced the formation of both HP1- and H3mK9-containing heterochromatic foci, which are characteristic of senescent cells (Figure 3C).

Proliferation was then assessed by a BrdU incorporation assay, which labels cells in the S phase. Forty-eight hours following lamin B1 transfection of WT primary fibroblasts, we observed a reduction in the proportion of cells transitioning through S phase, from 41.5–63.9% in empty vector-transfected cells to 16.8–18.5% in lamin B1-transfected cells (Figure 3D, left panel). This loss of proliferation was confirmed by a decrease of cyclin A protein, which regulates the S-phase transition, in fibroblasts transfected with the lamin B1 expression vector compared with fibroblasts transfected with empty vector (Figure 3D, right panel).

Taken together, these data show that lamin B1 overexpression alone is sufficient to induce senescence in WT primary fibroblasts, as evident by three different parameters: cell proliferation loss, SA-β-gal activity and SAHF.

Notably, although lamin B1 overexpression induced senescence, it did not activate DDR. Indeed, western blot analysis showed no changes in γ-H2AX, Chk1, Chk2 activation 48 h after transfection, which corresponds to the time of senescence detection (Supplementary Figure S3A). Similarly, the frequency of cells with γ-H2AX foci was not affected upon lamin B1 overexpression (Supplementary Figure S3B). This result suggests that lamin B1 overexpression does not induce senescence through DNA damage.

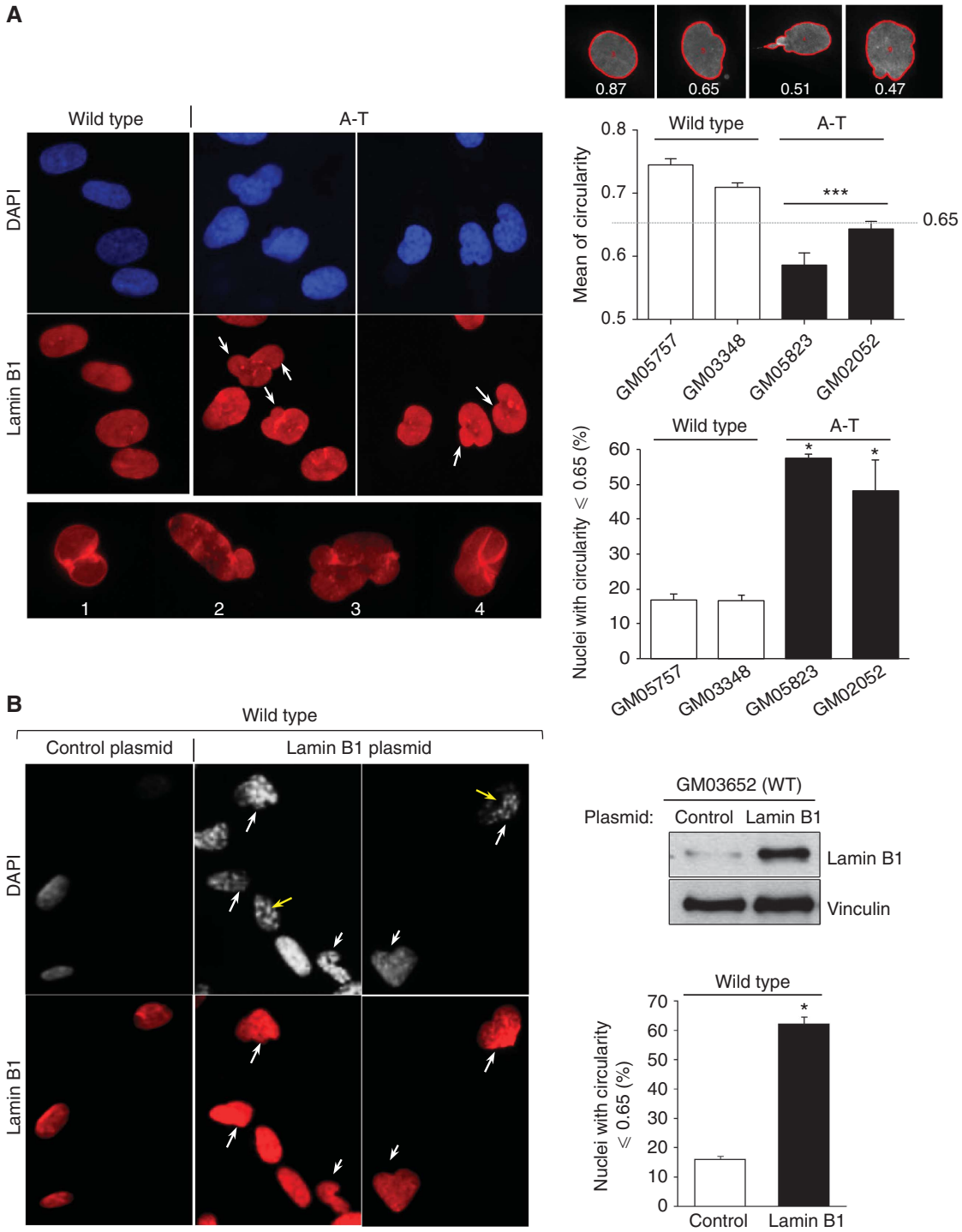

Figure 2 Frequency of mishappen nuclei in A-T cells and lamin B1-overexpressing cells. (**A**) The nuclear shapes of WT (GM05757, p17; GM03348, p15) and A-T (GM02052, p15; GM05823, p17) human primary fibroblasts examined by immunofluorescence with anti-lamin B1 (red) and DAPI (blue) (left panels). White arrows and lower panels show examples of alterations in nuclear morphology; nuclear envelope lobulations (1), nuclear blebbing (2 and 3), or crumpled nuclei (4) were observed in A-T cells. Right panels: analysis of nuclear circularity with Cellprofiler software. The upper panels show examples of values of circularity for the normal nucleus shape (left) and abnormal nuclear shapes (middle and right). The red line indicates the cell contour determined by the software. This analysis indicates that all nuclei with a circularity value $\leqslant 0.65$ have an abnormal shape. Middle panel: mean circularity in two WT and two AT primary fibroblast populations from three independent experiments. At least 100 nuclei were analysed. The values correspond to means from three independent experiments. ***Represents $P<0.0001$ (*t*-test). The error bars denote the s.e.m. Lower panel: percentage of cells with deformed nuclei (circularity $\leqslant 0.65$) from three independent experiments. (**B**) Abnormal shapes of nuclei in WT cells overexpressing lamin B1. Human wild-type (GM03652, p15) primary fibroblasts transfected with a lamin B1 expression vector compared with cells transfected with an empty expression vector (control) 48 h after transfection. Nuclear shape was determined as in (**A**) by immunofluorescence with anti-lamin B1 (red) and DAPI (grey). Yellow arrows show cells with senescence-associated heterochromatin foci (SAHF). Right upper panel: western blot of lamin B1 and actin on extract from wild-type primary fibroblasts transfected with the control or lamin B1 plasmid. Right lower panel: the values on the histogram correspond to the percentage of nuclei with circularity $\leqslant 0.65$ from three independent experiments. Nuclear shape analysis was performed on at least 100 cells per condition. *Represents a statistically significant difference ($P<0.05$). The error bars denote the s.e.m.

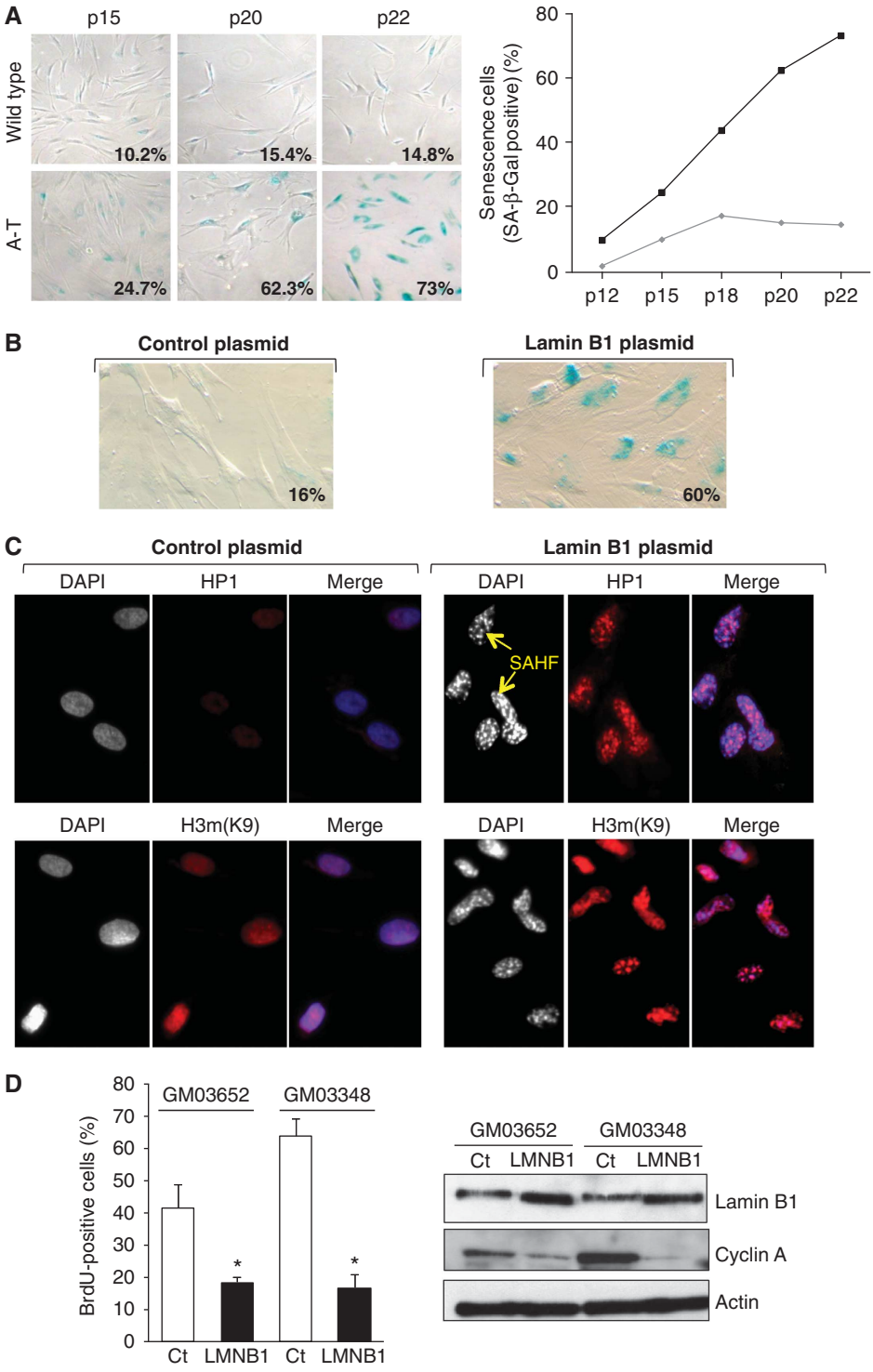

Figure 3 Lamin B1 overexpression induces senescence in primary fibroblasts. (**A**) Accelerated senescence in A-T cells. SA-β-galactosidase expression in WT (GM03652) and A-T (GM02052) primary fibroblasts as a function of passage. Representative photomicrographs of WT and A-T cells at the same magnification are shown. Right panel: quantification of SA-β-gal expression in WT (GM03652, grey diamonds) versus A-T (GM02052, black square) primary fibroblasts are shown. (**B**) SA-β-gal assay performed on WT primary fibroblasts (GM03652 at passage 15) 48 h after transfection of the control plasmid (left panels) or the lamin B1 plasmid (right panels). (**C**) Senescence-associated heterochromatin foci (SAHF) formation. The cells were stained 48 h after transfection. Yellow arrows: representative examples of SAHF. The merge shows an accumulation of HP1 and H3mK9 staining in condensed chromatin. (**D**) Effect of lamin B1 overexpression on BrdU incorporation. WT primary fibroblasts were transfected with an empty expression vector (Ct) or a lamin B1 expressing vector (LMNB1). Forty-eight hours following transfection, the cells were incubated for 24 h with 10 μM BrdU. The histogram represents the quantification of BrdU-positive cells. The values correspond to the means from three independent experiments. *Represents a statistically significant difference ($P<0.05$). Right panels: proteins were extracted 48 h after transfection and lamin B1, cyclin A and actin were detected by immunoblotting.

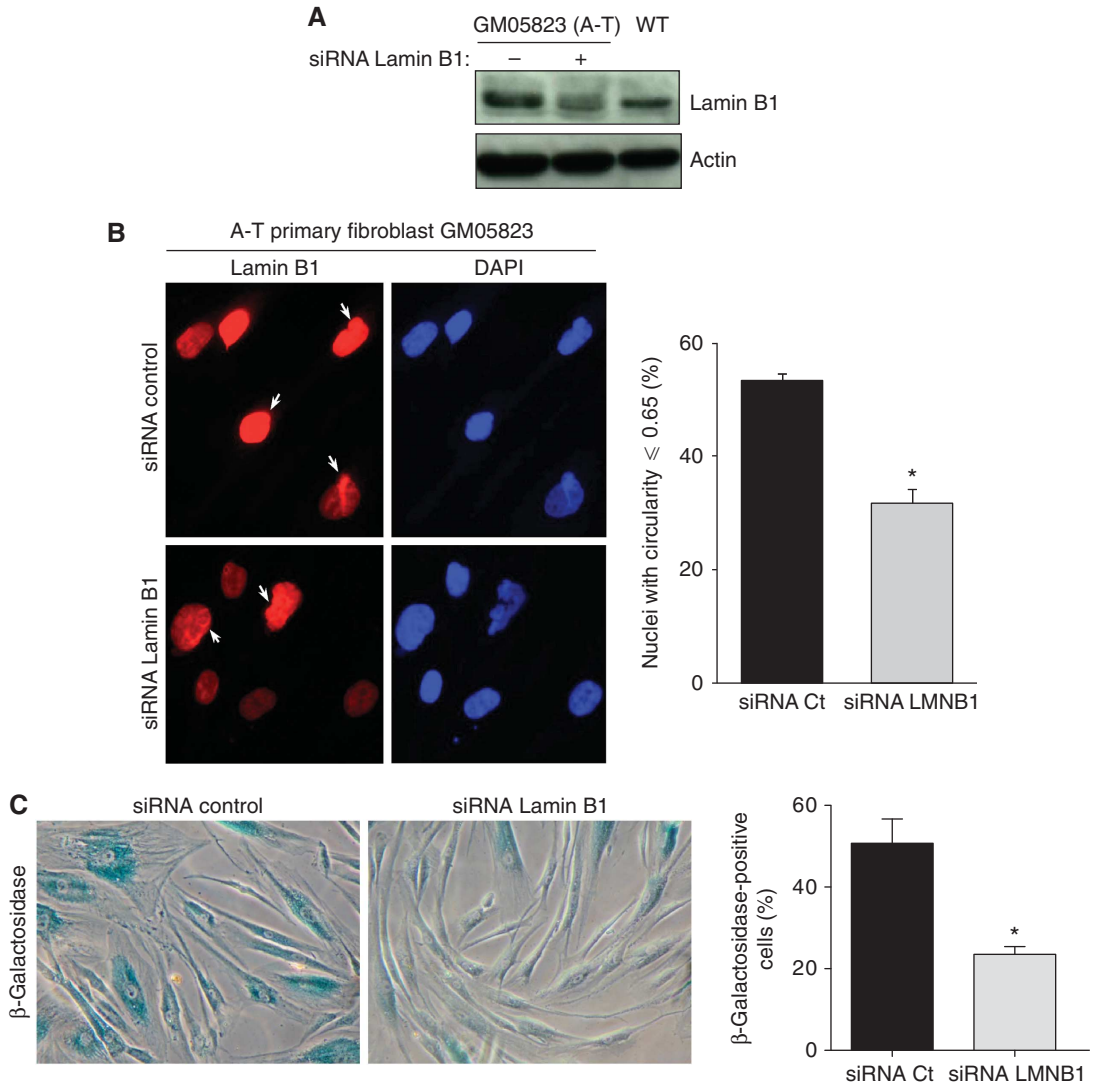

Figure 4 Reduction of the lamin B1 levels rescues nuclear shape alteration and senescence in A-T primary fibroblasts. (**A**) Western blot analysis of lamin B1 in extract from A-T primary fibroblasts transfected with control or lamin B1 siRNA (20 nM). (**B**) The alterations in nuclear shape in A-T human primary fibroblasts transfected with control or lamin B1 siRNA were examined by immunofluorescence with anti-lamin B1 (red) and DAPI (blue) 72 h following transfection (left panel). Right panel: % of misshapen nuclei (circularity $\leqslant$0.65) from three independent experiments. Nuclear shape analysis was performed on at least 100 cells per condition. (**C**) The SA-β-gal assay was performed on A-T human primary fibroblasts (GM05823) 72 h after transfection with control or lamin B1 siRNA. Histograms represent the quantification of SA-β-gal-positive cells from more than five randomly chosen fields ($\times$10 magnification). *Represents a statistically significant difference ($P<0.05$). Error bars denote the s.e.m.

An increase in lamin B1 is responsible for nuclear shape alterations and senescence in A-T cells

Because lamin B1 is spontaneously overexpressed in A-T cells and because lamin B1 overexpression is sufficient to induce senescence, we tested whether lamin B1 is responsible for senescence in A-T cells. Lamin B1 levels were decreased by RNA interference. Decreasing the level of lamin B1 below the basal level in WT cells could induce nuclear morphology alterations and potentially senescence (as reported by Vergnes *et al*, 2004 and Lammerding *et al*, 2006). Interestingly, we were able to establish conditions that reduced lamin B1 to levels comparable to that of WT cells (Figure 4A). Such conditions decreased both the frequency of cells with an altered nuclear shape from 53.4 to 31.7% and the frequency of senescent cells measured by the SA-β-gal activity assay from 50.7 to 23.5% (Figure 4B and C). These data show that lamin B1 is involved in nuclear alteration and senescence in A-T cells.

OS leads to an increase in lamin B1 and misshapen nuclei

Since high levels of endogenous OS may be responsible for many phenotypes of A-T patients, including premature ageing (Barzilai *et al*, 2002; Browne *et al*, 2004; Schubert *et al*, 2004; Reliene and Schiestl, 2006, 2007; Lavin *et al*, 2007; Reliene *et al*, 2008), we investigated whether OS is responsible for the increased levels of lamin B1 and nuclear malformation.

Treatment of WT cells with the pro-oxidants H_2O_2 or L-buthionine sulfoximine (BSO) (which depletes the glutathione pool) increased lamin B1 levels 2- to 5- to 9-fold in lymphoblasts and 2.9-fold in primary fibroblasts. Reciprocally, treatment of A-T cells with the antioxidant

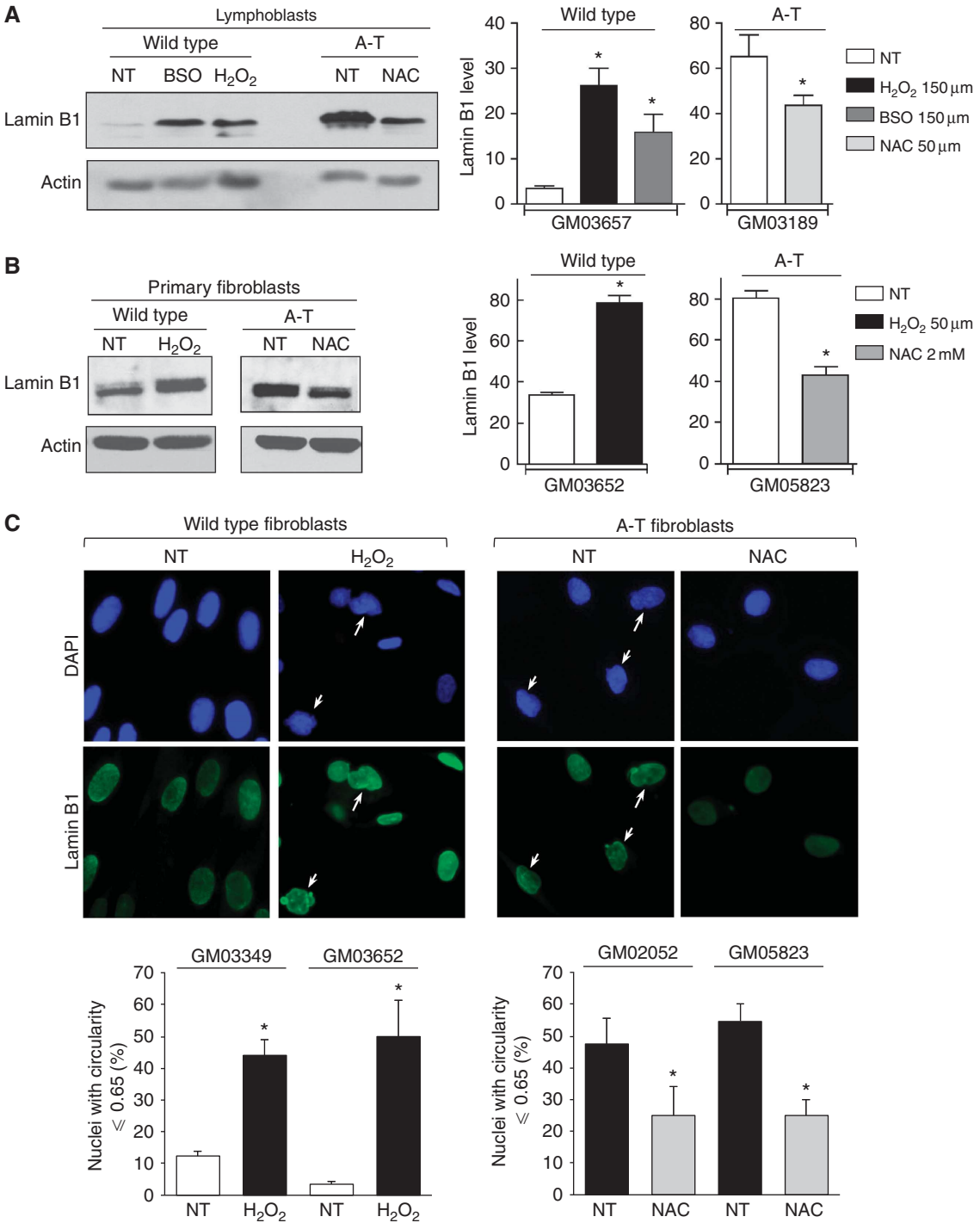

Figure 5 Effect of oxidative stress on lamin B1 levels and nuclear morphology. (**A**) WT and A-T lymphoblasts were treated with H_2O_2 or BSO and NAC, respectively. (**B**) WT and A-T primary fibroblasts were treated with H_2O_2 and NAC, respectively. Upper right panels: quantification of lamin B1 levels relative to actin following treatment. The values correspond to the means of three to eight independent experiments. *Represents a statistically significant difference ($P<0.05$) between untreated (NT) and treated cells. The error bars denote the s.e.m. (**C**) Impact of oxidative stress on nuclear shape. Upper panels: WT and A-T fibroblasts were treated with H_2O_2 and NAC, respectively, for 72 h and analysed by immunofluorescence with anti-lamin B1 (green) and DAPI (blue). White arrows: alterations in nuclear morphology (white arrows). Lower panels: quantification of abnormal nuclei. Means from three separate experiments are expressed after H_2O_2 treatment in wild-type primary fibroblasts (GM03349 p14 and GM03652 p14, left panel) and after NAC treatment in A-T primary fibroblasts (GM2052 p14 and GM05823 p18, right panel). At least 150 cells were counted per group. *Represents a statistically significant difference ($P<0.05$) between untreated (NT) versus treated cells. The error bars denote the s.e.m.

N-acetyl-L-cysteine (NAC) significantly reduced lamin B1 levels (Figure 5A and B). These data show that OS leads to lamin B1 accumulation. NAC also affected lamin B1 levels in WT primary fibroblasts, reflecting endogenous ROS (Supplementary Figure S4A). Of note, in A-T cells, lamin A/C levels were not affected by antioxidant treatment

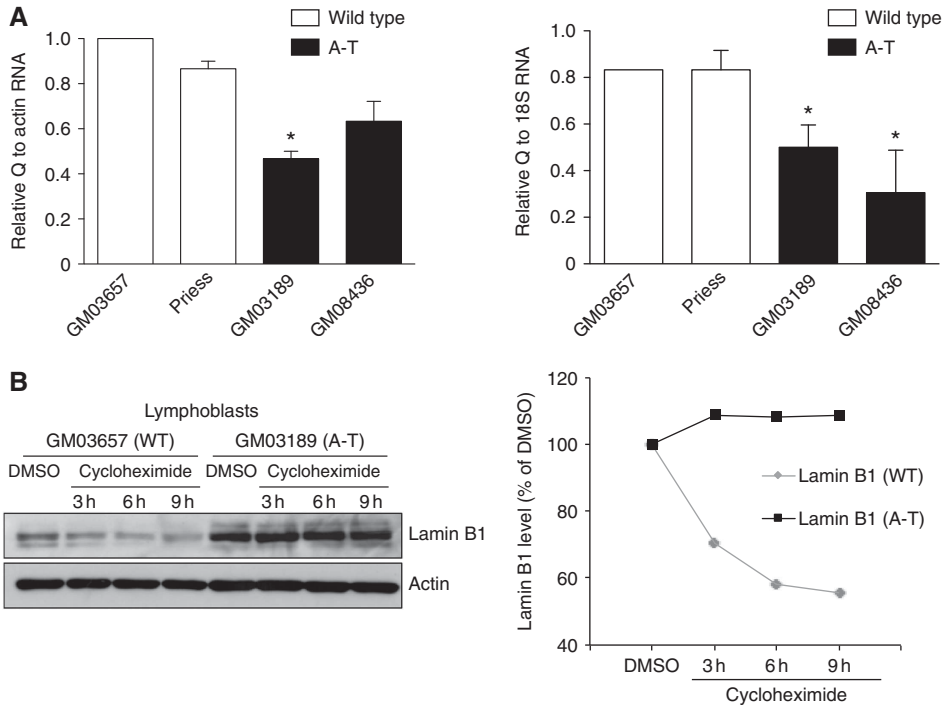

Figure 6 Expression and stability of lamin B1 in WT versus A-T cells. (**A**) mRNA levels by real-time PCR quantification. A parallel amplification using the ACTIN and 18S rRNA primers was carried out as a reference. The values correspond to the means from three independent experiments. *Represents a statistically significant difference ($P \leqslant 0.05$). Error bars denote the s.e.m. (**B**) The stability of lamin B1 in WT (GM03657) versus A-T (GM03189) cells was analysed by western blot after 3, 6 or 9 h of 50 μg/ml cycloheximide treatment.

(Supplementary Figure S4B), suggesting that endogenous ROS specially affects lamin B1.

Because pro-oxidant treatment induced the accumulation of the lamin B1 protein, we tested whether it also affects nuclear shape. Indeed, H_2O_2 treatment of WT primary fibroblasts led to nuclear alterations (from 12.4 to 44.1% and from 3.5 to 50% in GM3349 and GM03652 cells, respectively) (Figure 5C, left panel), consistently with the impact of lamin B1 overexpression. Conversely, NAC treatment rescued nuclear shape in A-T cells (from 47.5 to 25% and from 54.6 to 25% in GM02052 and GM05823 cells, respectively) (Figure 5C, right panel).

Taken together, these data show that OS leads to the accumulation of lamin B1 and to nuclear morphology alteration.

The lamin B1 protein is stabilized in A-T cells

Real-time PCR analysis did not reveal an increase of lamin B1 mRNA in A-T cells but showed a decrease (Figure 6A). This suggests that the increase in the lamin B1 protein level likely results from post-transcriptional protein stabilization rather than from transcriptional stimulation of the *LMNB1* gene, which encodes lamin B1. Because lamin B1 is increased at the protein level (see data above), the decrease of lamin B1 mRNA observed in A-T cells may result from a negative feedback regulation loop, as suggested previously (Lin and Fu, 2009). Therefore, we investigated the stability of the lamin B1 protein in A-T cells compared with WT cells. Cycloheximide treatment led to a decrease of lamin B1 protein levels in WT cells after 3 h of treatment, whereas lamin B1 protein levels remained unaffected in A-T cells even after 9 h (Figure 6B; Supplementary Figure S5A). Notably, the stabilization did not result from a difference in the regulation of apoptosis because similar data were obtained in the presence of the apoptosis inhibitor Z-VAD (Supplementary Figure S5B). Treatment with the proteasome inhibitor MG132 increased the level of lamin B1 protein in WT cells, suggesting that at least part of the regulation of lamin B1 turnover involved in the proteosomal pathway (Supplementary Figure S5C). In contrast, treatment with leupeptin, a lyzosome inhibitor, did not have any effect.

Together, these data show that the stability of the lamin B1 protein is increased in A-T cells.

p38 MAPK activation leads to lamin B1 accumulation

We next investigated the cellular pathway that could lead to the accumulation of lamin B1 in A-T cells or after OS. p38 MAPK was a good candidate for three reasons: (1) p38 MAPK is a kinase activated by OS; (2) it is activated in senescence induced by different stresses (Wang *et al*, 2002; Iwasa *et al*, 2003; Torres and Forman, 2003; Matsuzawa and Ichijo, 2008; Pan *et al*, 2009; Freund *et al*, 2011) and (3) it is part of an ATM-independent pathway of senescence (Naka *et al*, 2004).

To test for the possible role of p38 MAPK, we first measured the spontaneous activation of p38 MAPK in A-T versus WT cells using specific antibodies against phospho(T180-Y182)-p38 MAPK, that is, the active form of p38 MAPK. We observed a higher level of activated p38 MAPK in A-T compared with WT extracts (Supplementary Figure S6A and B). These observations are consistent with the high level of spontaneous ROS in A-T cells. Consistently, the kinase p38 MAPK activity was increased in A-T cells compared with WT cells. Indeed, the specific substrate, ATF2, was more efficiently phosphorylated when P-p38

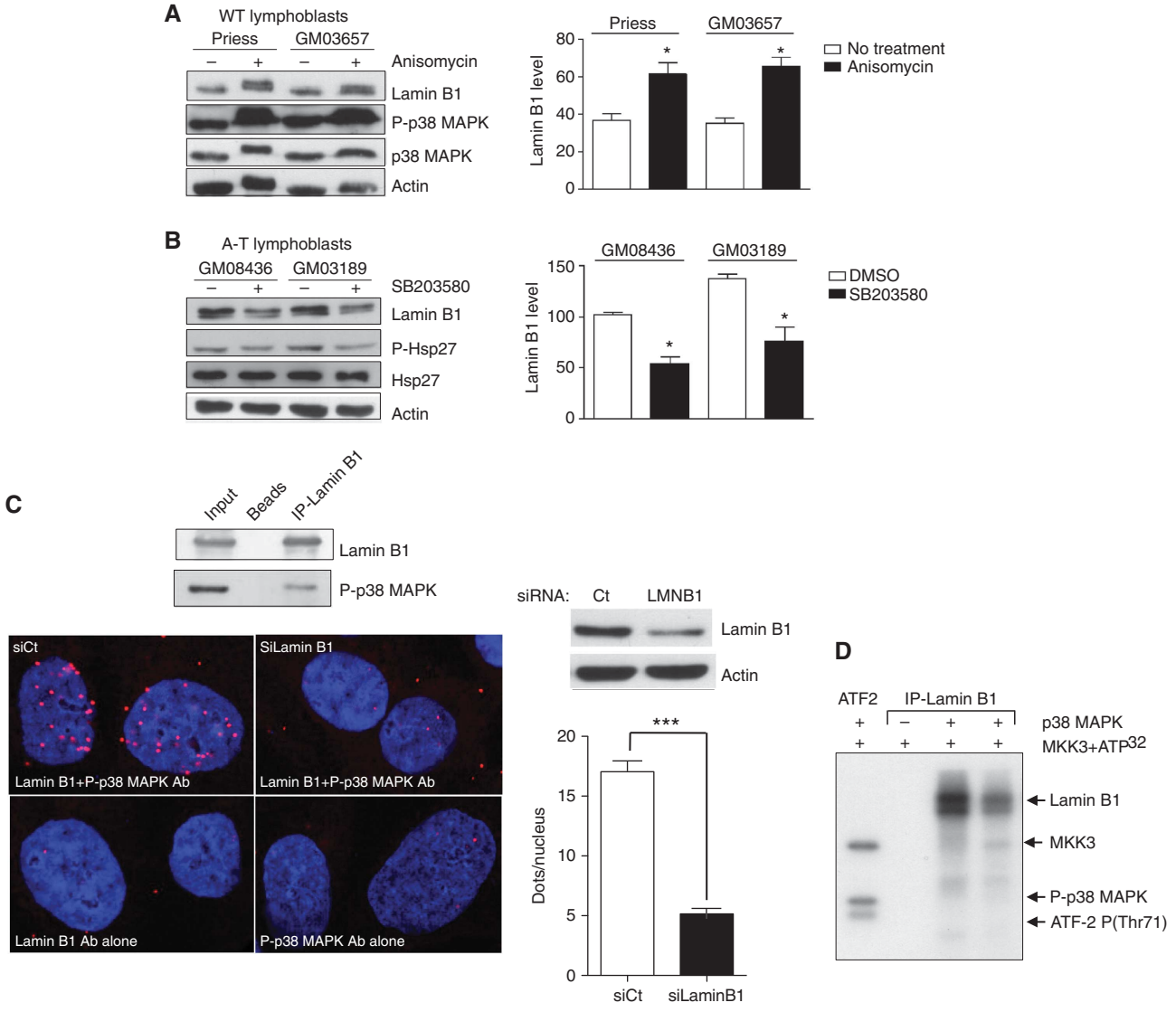

Figure 7 Impact of p38 MAPK on lamin B1 levels and interactions between p38 MAPK and lamin B1. Modifications of lamin B1 levels after anisomycin (**A**) or SB203580 (**B**) treatment. Left panels: western blot analysis after 24 h of anisomycin (10 μg/ml) or SB203580 (10 μM) treatment. Right panels: quantification of lamin B1 after anisomycin (**A**) or SB203580 (**B**) treatment. Immunoblotting of P(T180-Y182)-p38 MAPK and P-(Ser82)-Hsp27 protein, a substrate of p38 MAPK, was performed to confirm the efficiency of anisomycin and inhibitor SB203580, respectively, on p38 MAPK activity. (**C**) Upper panel: co-immunoprecipitation of lamin B1 (overexpressed 48 h before protein extraction) and endogenous P-p38 MAPK. Lower panels: *in-situ* interactions between endogenous lamin B1 and activated p38 MAPK monitored by the proximity ligation assay (PLA) using the anti-P(T180/Y182)-p38 MAPK and lamin B1 (bottom panel) antibodies. Proximal locations between the two proteins were observed as red fluorescent dots. Right upper panel: a western blot showing the efficiency of lamin B1 siRNA 48 h after treatment. Right lower panel: quantification of *in-situ* PLA in cells transfected with negative control siRNA (siCtrl) or with lamin B1 siRNA (siLMNB1). Each value represents the mean number of dots in >155 nuclei. *Represents a statistically significant difference ($P<0.05$). ***Represents $P<0.0001$ (*t*-test). The error bars denote the s.e.m. (**D**) *In-vitro* phosphorylation of lamin B1 by p38 MAPK on SV-40 fibroblasts. The kinase activity of p38 MAPK on immunoprecipitated lamin B1 protein from two WT lymphoblasts protein extracts (Priess and GM03657) was evaluated by a radioactive assay. In the presence of MKK3 (a p38 MAPK activator) and ^{32P}ATP, p38 MAPK phosphorylated lamin B1 *in vitro* (lanes 3 and 4). In the first lane, ATF2-P(T71), a specific substrate of p38 MAPK, served as a positive control of p38 MAPK activity. In the second lane, no lamin B1 phosphorylation was detected in the absence of p38 MAPK.

MAPK was immunoprecipitated from A-T cells than from WT cells (Supplementary Figure S6B).

The activation of p38 MAPK in unchallenged A-T cells could be due to endogenous OS, as reported in haematopoietic stem cells from $atm^{(-/-)}$ mice (Ito *et al*, 2006). Indeed, treatment of A-T cells with the antioxidant NAC significantly reduced the level of activated p38 MAPK; reciprocally, the level of activated p38 MAPK increased after treatment of WT fibroblasts with the pro-oxidant H_2O_2 (Supplementary Figure S6C).

To test whether p38 MAPK activation affects lamin B1 levels, WT cells were treated with anisomycin, an MAPK activator, and A-T cells with SB203580, a p38 MAPK inhibitor. Activation of p38 MAPK significantly increased lamin B1 levels in WT cells (Figure 7A; Supplementary Figure S6D), whereas inhibition of p38 MAPK decreased the lamin B1 level in A-T cells (Figure 7B).

Taken together, these data show that p38 MAPK activation leads to the accumulation of lamin B1 protein and suggest that p38 MAPK is a key player in the process leading to lamin

B1 accumulation in A-T cells, which led us to test for a potential interaction between lamin B1 and p38 MAPK.

In-vitro phosphorylation of lamin B1 by p38 MAPK

Lamin B1 immunoprecipitation resulted in the co-immunoprecipitation of P-p38 MAPK (Figure 7C, upper panel). We confirmed the lamin B1–p38 MAPK interaction by the proximity ligation assay (PLA), which allows the *in-situ* detection of endogenous protein interactions by immunofluorescence microscopy (Fredriksson *et al*, 2002; Soderberg *et al*, 2006, 2008; Laulier *et al*, 2011). Fluorescent interaction spots were visible only when both primary antibodies were simultaneously used. Notably, this interaction was nearly abolished when cells were transfected with siRNA against lamin B1, showing the specificity of the interaction between lamin B1 and p38 MAPK (Figure 7C, lower panel). Together, these data demonstrated a physical interaction between lamin B1 and p38 MAPK.

Importantly, we next showed that activated recombinant p38 MAPK was able to phosphorylate lamin B1 *in vitro* (Figure 7D).

Taken together, these data suggest that p38 MAPK participate in the induction of senescence after OS by influencing the level of lamin B1 protein. To address this hypothesis, we treated cells with H_2O_2 in the presence or absence of the p38 inhibitor SB203580 and measured lamin B1 levels and senescence. The increase in lamin B1 protein levels by H_2O_2 was accompanied by an induction of senescence (Supplementary Figure S7A). Importantly, in the presence of the p38 inhibitor, treatment with H_2O_2 failed to increase both lamin B1 levels and senescence (Supplementary Figure S7B).

These data show that OS increases lamin B1 and senescence through p38 MAPK activation.

Inhibition of p38 MAPK in A-T cells prevents lamin B1 protein accumulation, nuclear alterations and senescence

Finally, to directly assess the impact of the p38 MAPK-lamin B1 pathway on the alteration of nuclear shape and senescence in A-T cells, p38 MAPK was silenced by RNA interference. Even a partial loss of p38 MAPK led to two- to three-fold reduction of lamin B1 protein levels in A-T primary fibroblasts (Figure 8A), consistent with the data using the SB203580 inhibitor (compare Figures 8A and 7B). Interestingly, silencing of p38 MAPK in A-T cells also led to a reduction in the frequency of cells with alterations in nuclear shape from 56.1 and 60.4% in cells transfected with the control siRNA to 27.8 and 30.1% cells transfected with the p38 siRNA (Figure 8B) and concomitantly to a reduction in the frequency of senescent cells (Figure 8C).

Together, these data showed that p38 MAPK activation increased the cellular level of endogenous lamin B1, which leads to alterations in nuclear shape and to senescence in A-T cells, in an ATM-independent manner.

Discussion

A-T has a complex clinical profile, comprising phenotypes resulting from DDR defects (radiation sensitivity, genetic instability and predisposition to cancer), neurological disorders and premature ageing (Lavin, 2008). Although ATM regulates telomeric maintenance, h-TERT-expressing A-T fibroblasts show premature senescence, demonstrating that the senescence of A-T cells is not completely due to telomeric shortening (Naka *et al*, 2004). The ATM kinase regulates a network of multiple pathways controlling DDR, the response to ROS and senescence induced by hyper-replication, DNA damage and OIS. However, the limited role played by ATM in OIS in mice (Efeyan *et al*, 2009) and the evidence that A-T cells maintain senescent phenotypes argue for the existence of an alternative senescence pathway. Both ATM and p38 MAPK participate in stress-induced senescence via two parallel pathways, and p38 MAPK could be responsible for senescence in A-T, but the underlying molecular mechanisms remain uncharacterized (Naka *et al*, 2004). Here, we detailed a senescence-inducing pathway in AT cells thus independent of ATM. We showed that in response to ROS, activation of p38 MAPK increased the cellular level of endogenous lamin B1 and that a high lamin B1 level led to nuclear shape alterations and senescence. Thus, in an ATM-alternative pathway, lamin B1 appears to be a pivotal molecular effector, for OS to induce nuclear architecture alteration through p38 MAPK. Notably, ROS and p38 MAPK are induced by two canonical situations leading to senescence, which constitute two paradigms of senescence induction: OIS and stress-induced senescence (Lee *et al*, 1999; Iwasa *et al*, 2003; Han and Sun, 2007; Lu and Finkel, 2008). Interestingly, we also showed that nuclear shape alterations and lamin B1 accumulation were also induced during these two canonical situations (Supplementary Figure S8), showing that lamin B1 accumulation is not restricted to A-T but is more generally associated with senescence in response to ROS induction. Thus, it is tempting to propose that lamin B1 is a general mediator and marker of OS-induced senescence.

Notably, high levels of endogenous OS can be responsible for many A-T phenotypes (Barzilai *et al*, 2002; Browne *et al*, 2004; Ito *et al*, 2007; Lavin *et al*, 2007; Reliene and Schiestl, 2007; Reliene *et al*, 2008). Therefore, the existence of the OS-induced senescence pathway described here provides additional molecular arguments in favour of treating A-T patients with antioxidants (Lavin *et al*, 2007) and opens new avenues by identifying the p38-lamin B1 pathway as a possible additional therapeutic target.

Many processes can lead to senescence, including DDR defects, OS, and alterations of nuclear architecture. However, the putative relationships between these three processes have been poorly documented. In our study, A-T cells associated with the three aforementioned defects. Until now, progeroid syndromes have been classified into two distinct categories: laminopathies, in which lamins are altered, and DDR defect syndromes (Lans and Hoeijmakers, 2006). Because our data showed an increase of lamin B1 levels and modification of nuclear architecture in A-T cells, this pathology can describe both classes of progeroid syndromes. Notably, these two defects may potentiate each other. Indeed, dysregulation of lamin A/C affect DNA damage signalling and genomic stability in laminopathies (Liu *et al*, 2005, 2006; Misteli and Scaffidi, 2005; Manju *et al*, 2006; Parnaik and Manju, 2006; di Masi *et al*, 2008; Liu and Zhou, 2008; Gonzalez-Suarez *et al*, 2009a, b; Redwood *et al*, 2011). Thus, it is tempting to speculate that the overexpression of lamin B1 similarly affects DNA metabolism.

Duplication of the *LMNB1* gene, resulting in lamin B1 overexpression, has been described in adult-onset autosomal

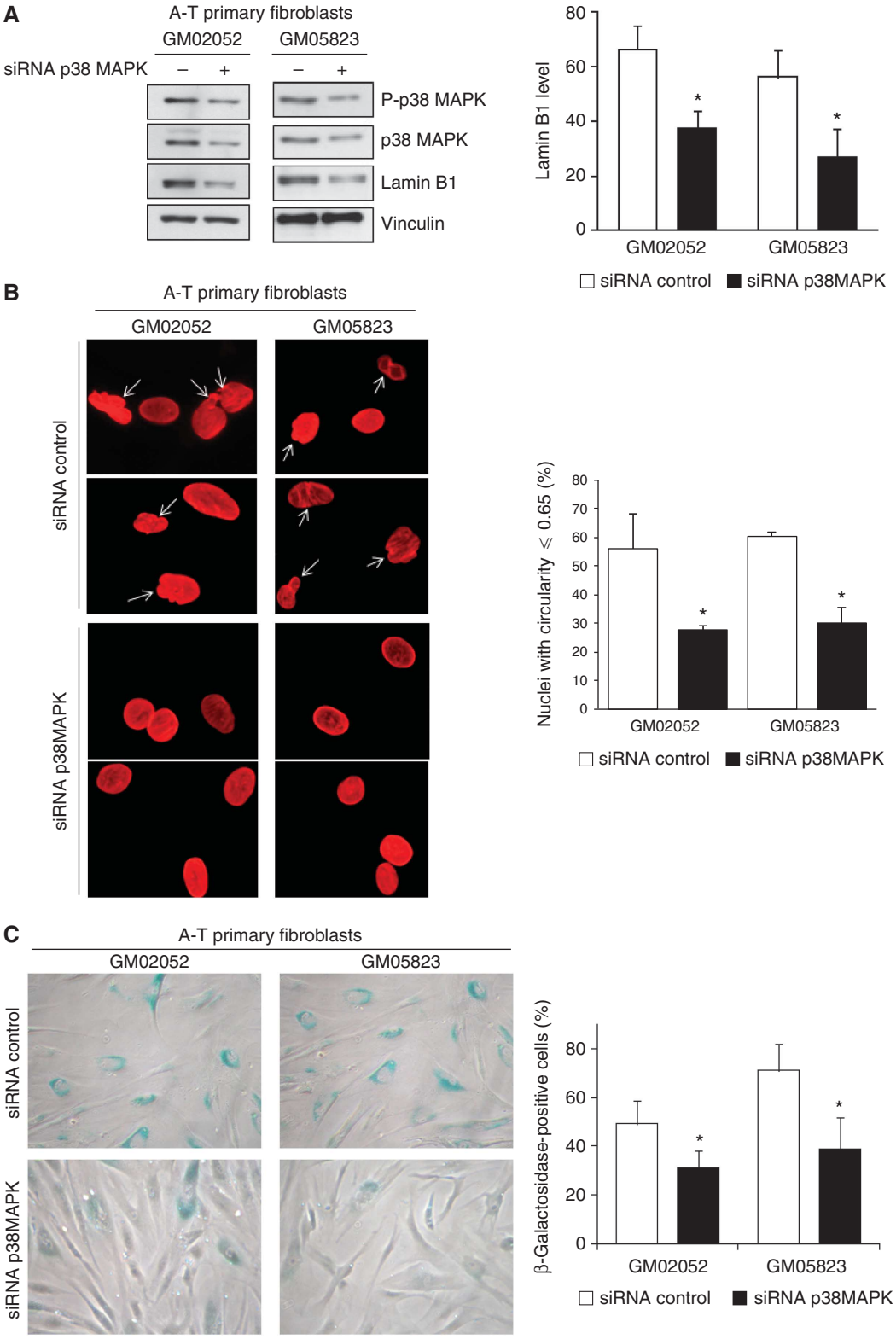

Figure 8 Impact of silencing p38 MAPK in A-T primary fibroblasts. (**A**) Impact of siRNA p38 MAPK (40 nM) on lamin B1 levels. Left panel: western blot analysis. Right panels: quantification of lamin B1 levels after treatment. The values correspond to the means from three independent experiments. *Represents a statistically significant difference ($P<0.05$) between control and p38 MAPK siRNA-treated cells. Error bars denote the s.e.m. (**B**) Impact on nuclear shape. Left panels: nuclear shape of A-T fibroblasts that were treated for 72 h with control and p38 MAPK siRNA and analysed by immunofluorescence with anti-lamin B1 (red). Right panel: quantification of abnormal nuclei: circularity $\leqslant 0.65$ (white arrows). The data are the means from three independent experiments. At least 150 cells were counted per group. *Represents a statistically significant difference ($P<0.05$). The error bars denote the s.e.m. (**C**) Impact on senescence in A-T primary fibroblasts. SA-β-galactosidase expression in A-T primary fibroblasts was analysed 72 h after siRNA transfection. Left panels: representative photomicrographs. Right panel: quantification of SA-β-gal expression following control or p38 MAPK siRNA treatment. SA-β-gal-positive cells were quantified from more than five randomly chosen fields (× 10 magnification). The mean values from three separate experiments are presented. *Represents a statistically significant difference ($P<0.05$) between the control and p38 MAPK siRNA-treated cells. Error bars denote the s.e.m.

dominant leukodystrophy (ADLD) (Padiath *et al*, 2006; Meijer *et al*, 2008). Interestingly, lamin B1 and lamin B2 deficiencies are associated with other neurological defects, indicating that the level of lamin B1 must be very tightly controlled to avoid both defects and excess levels (Coffinier *et al*, 2011). Published observations show that defect in lamin B1 leads to nuclear morphology alterations (Vergnes *et al*, 2004; Lammerding *et al*, 2006). Our data show that lamin B1 can also be indirectly dysregulated due to a mutation in ATM. Remarkably, A-T and ADLD share common clinical traits, such as the demyelination of the central nervous system (CNS), which is associated with severe neurological defects. The molecular causes of the CNS demyelination and neurological defects in A-T remain puzzling (Barzilai *et al*, 2008; Biton *et al*, 2008). Supported by a recent report demonstrating that *LMNB1* overexpression affects the expression of myelin synthesis genes thereby causing CNS demyelination (Lin and Fu, 2009), our data thus provide a potential molecular explanation for the neurological disorders in A-T. Therefore, in parallel to DDR defects, lamin B1 overexpression could account for important clinical traits of A-T, including premature ageing and CNS defects/neurological disorders. More generally, lamin B1 overexpression could explain the neurological defects and/or senescence phenotypes in different disorders associated with elevated OS.

Cell viability in response to OS requires regulation of the redox balance. The transcription factor Oct1 regulates this balance by inhibiting the transcription of detoxification genes, such as *PRDX2*, *GPX3* and *SOD1*. The retention of Oct1 at the nuclear periphery allows these genes to be expressed and consequently improves cell viability under OS (Tantin *et al*, 2005; Malhas and Vaux, 2009). Importantly, lamin B1 is required for Oct1 localization at the nuclear periphery, and loss of lamin B1 leads to a higher sensitivity to OS (Malhas *et al*, 2009). Because our study showed that OS increased lamin B1 protein levels, these data collectively support a model in which lamin B1 accumulates in response to OS to protect cells against OS. We confirmed this model by showing that lamin B1 overexpression decreases both basal and H_2O_2-induced ROS levels and increases cell survival in response to OS exposure (Supplementary Figure S9). Thus, lamin B1 overexpression participates in the endogenous cell response to OS. p38 MAPK is generally believed to be a kinase that mediates cell death. In contrast, some studies found that activation of p38 MAPK by stress stimuli may not necessarily promote cell death; instead, it could enhance cell survival by mechanisms that are still poorly characterized (Thornton and Rincon, 2009). Our data shed light on the molecular pathway by which p38 MAPK can control the expression of detoxification genes via lamin B1 accumulation, which can underlie a prosurvival function of p38 MAPK.

The present data can be unified in the following model (Figure 9): (1) OS activates p38 MAPK; (2) p38 MAPK activation leads to high levels of the lamin B1 protein, which is part of the cellular response to OS; (3) accumulation of lamin B1 decreases the level of ROS, thereby increasing the resistance of cells to OS; and (4) in the case of persistent and chronic OS (e.g., in genetic diseases such as A-T), prolonged high levels of lamin B1 affect both the nuclear architecture, thereby triggering senescence (present data), and the expression of myelin synthesis genes, resulting in neurological disorders (Lin and Fu, 2009). Our results highlight the missing link at the crossroads between OS, the alteration of nuclear architecture and senescence and identify lamin B1 as a key mediator of senescence in response to OS.

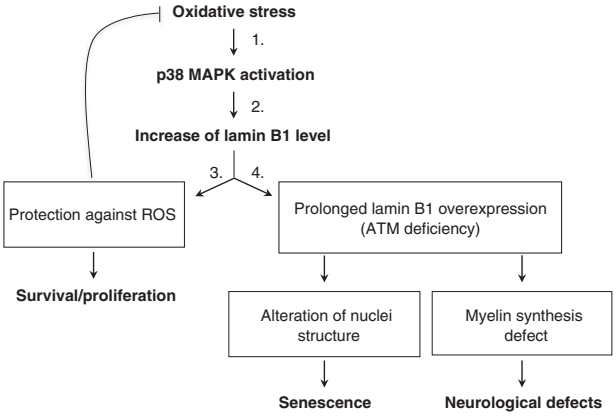

Figure 9 Consequences of lamin B1 accumulation on redox balance, senescence and neurological defects. Oxidative stress leads to an increase of levels of lamin B1 through activation of p38 MAPK. Our data show an important role for lamin B1 protein in the control of oxidative stress, by regulating the ROS levels and improving cell viability. In case of persistent oxidative stress (such as in A-T cells), prolonged accumulation of lamin B1 levels leads to senescence and/or neurological defects. Indeed, lamin B1 can impact on nuclear architecture morphology and senescence, as shown in the present report, as well as on myelin gene synthesis as it was reported in Lin and Fu (2009).

Materials and methods

Cell culture, treatments and transfection

Cells were grown at 37°C with 5% CO_2 in Modified Eagle's medium. Human primary fibroblasts were grown in MEM (Invitrogen, Carlsbad, USA), lymphoblasts in RPMI-1640 (Lonza Group Ltd., Switzerland) supplemented both with 20% fetal calf serum (FCS; Lonza Group Ltd.) and SV-40 human primary fibroblasts in DMEM supplemented with 10% FCS. All media were supplemented with 2 mM glutamine, 200 IU/ml penicillin, and 100 mg/ml streptomycin (Calbiochem, Merck Biosciences, Darmstadt, Germany). For prooxidant treatment, normal primary fibroblasts were exposed to 50 μM H_2O_2 at 37°C in culture for 72 h. WT lymphoblasts were exposed to 100 μM H_2O_2 at 37°C in culture for 24 h. For antioxidant treatment, A-T primary fibroblasts and lymphoblasts were exposed to 2 mM NAC (Sigma-Aldrich, St Louis, MO, USA) for 48 and 24 h, respectively. p38 MAPK activation or inhibition on lamin B1 levels in lymphoblasts was assessed by 24 h of anisomycin (10 μg/ml, Sigma-Aldrich) or SB203580 (10 μM, Invitrogen) treatment, respectively. For inhibition of phospho-serine-1981 ATM, lymphoblasts were treated for 24 h with 10 μM KU-55933 (Cell Signaling, Ozyme, France). Nucleotransfection of primary fibroblasts was performed using the Amaxa Nucleofector System (Lonza Group Ltd.). Forty-eight hours after transfection of empty plasmid or human lamin B1 cDNA (Origene, Clinisciences SA, France) or 72 h of lamin B1 siRNA (Eurogentec, France), nuclear morphology analysis or the SA-β-gal assay was performed.

Western blot analysis

Cells were suspended in lysis buffer (8 M urea, 1 M thiourea, 4.8% CHAPS, 50 mM DTT, 24 mM spermine dehydrate, protease inhibitor cocktail (Complete Lysis Buffer; Roche, Meylan, France), and 0.1 mM Na_3VO_4). To fragment the DNA and then to improve the proteins extraction, repeated mechanical disruptions of lysate through a needle attached to 0.3 ml were performed. After incubation for 1 h at room temperature, samples were cleared by centrifugation at 100 000 *g* in a TLA-100 rotor (Beckman, Fullerton,

CA, USA). For each blot, equal amounts (30 μg) of protein were loaded per sample. Electrophoresis separation, transfer onto nitrocellulose membrane and antibody probing were performed using standard techniques. Proteins were visualized using the ECL Western Blotting System. Lamin B1 and B2 were probed with antibodies at 1:500 (Abcam Inc., Cambridge, UK), and actin was probed with specific antibody at 1:1000 (Sigma-Aldrich). The phosphorylated forms of ATM, Chk2, Hsp27 and p38 MAP kinases were detected, respectively, with anti-P(S1981)-ATM (Rockland, Bridgeport, USA) and anti-P(T68)-Chk2, anti-P(S82)-Hsp27 and anti-phospho(T180-Y182) p38 MAPK-MAPK (Cell Signaling Technology Inc., Danvers, MA, USA) antibodies at 1:500. Vinculin and PARP protein detection was performed using specific antibodies at 1:5000 (Abcam Inc. and Cell Signaling Technology Inc., respectively). Cyclin A was detected using specific antibody at 1:500 (Abcam Inc.).

Immunofluorescence microscopy

Cells were grown on glass coverslips, fixed with 2% paraformaldehyde or cold methanol and permeabilized with 0.5% saponin. After blocking, cells were incubated with anti-lamin B1, anti-HP1 or H3mK9 primary antibodies (Abcam Inc.) diluted in PBS containing 1% BSA and 0.05% Tween.

After washing with PBS containing 1% BSA, the cells were incubated with FITC-conjugated goat anti-mouse Ig or RHOD-conjugated goat-rabbit Ig (Jackson ImmunoResearch Laboratories, Inc., West Grove, PA, USA) and stained with DAPI. Finally, the slides were mounted with a fluorescent mounting medium (Fluoromount). Images were obtained with a $\times 40$ objective and processed with the fluo IMSTAR software (IMSTAR S.A., France).

Immunodetection of lamin B1 was performed on a Leica DM5500 microscope equipped with a CoolSNAP HQ CCD camera and $\times 63$ objective. Data acquisition was performed with MetaMorph (Universal Imaging). The lamin B1 fluorescence intensity per nucleus was measured with Image J Mean Gray Value Parameter.

In-situ PLA

Staining with primary antibodies was performed as described above for immunofluorescence microscopy using mouse phospho-p38 MAPK (Thr180/Tyr182) (Cell Signaling Technology Inc.) and rabbit lamin B1 (Abcam) antibodies. Then, *in-situ* PLA was performed using the Duolink II Fluorescence kit (OLINK Bioscience) according to manufacturer's protocol. Image acquisition was performed with a Leica DMRxA2 confocal microscope SPE (Leica Microsystems, Welzlar, Germany) using ACS APO $\times 63$ 1.3 oil lenses. Images were processed with the Leica and ImageJ software.

Nuclear shape measurements

CellProfiler image analysis software was used to measure cellular morphological parameters. Shape features of nuclei stained by lamin B1 were determined using the specific 'measure object size shape' module. Among these shape features, we focused on the Form Factor values (calculated as $4 \times \pi \times \text{Area}/\text{Perimeter}^2$) to quantify nuclei with abnormal shapes. A Form Factor equal to 1 corresponds to perfectly circular nuclei.

Cytochemical detection of SA-β-gal

SA-β-gal-positive cells were detected as previously described (Dimri *et al*, 1995). Briefly, monolayers of cells were fixed with 2% formaldehyde and 0.2% glutaraldehyde and incubated at 37°C in staining solution (Cell Signaling Technology Inc.). After overnight incubation, the percentage of stained cells was determined at $\times 10$ magnification with a Zeiss microscope (Statif Axio vertical 40C, Zeiss). SA-β-gal-positive cells were quantified from more than five randomly chosen fields.

BrdU staining

Cells were grown on coverslips, labelled for 24 h in 10 μm bromodeoxyuridine (BrdU) and fixed in cold methanol. DNA was denatured by incubating the cells in 4 N HCl for 20 min at RT, and BrdU staining was performed according to manufacturer's recommendations with FITC-conjugated anti-BrdU (Becton Dickinson). Nuclear DNA was counterstained with 1 μg/ml DAPI.

RNA interference

siRNA-specific lamin B1 (5′-AGAGUCUAGAGCAUGUUUG-3′) and control siRNA (NEG05, Eurogentec) were nucleofected using the Amaxa system according to manufacturer's conditions. A mix of two sequences of p38 MAPK siRNA (5′-GCACCAUGAAGAUCAA GAU-3′ and 5′-CCUUCCAGCAGAUGUGGAU-3′) were transfected into cells using INTERFERin (Polyplus Transfection, Illkirch, France) under conditions specified by the manufacturer.

Relative real-time PCR quantification

Quantitative PCR was carried out in a Mastercycler® ep realplex real-time PCR system (Eppendorf, France) using technical duplicates of three separate experiments for each primer on 10 ng/μl cDNA for LMNB1 and 0.1 and 0.01 ng/μl cDNA for the ACTIN and 18S reference genes, respectively. A parallel amplification using the ACTIN and 18S rRNA primers was carried out as a reference. In each case, duplicate threshold cycle (Ct) values were obtained and averaged. Lamin B1 expression was then determined by the relative quantification (Q) method.

Co-immunoprecipitation

Forty-eight hours following transfection of lamin B1 expression vector using Jet-PEI (Polyplus Transfection), SV40 fibroblasts were lysed in a 150-mM NaCl buffer (NaCl 150 mM, NP-40 1%, EDTA 1 mM, Tris 25 mM pH 7.5) containing phosphatases and protease inhibitors for 45 min on ice. To improve the efficiently of extraction, we repeated mechanical disruption by passing the lysate 10 times through a needle attached to a 0.3-ml syringe. After centrifugation at 13 000 *g* for 30 min at 4°C, lysates were precleared and incubated (250 μg proteins) overnight at 4°C under agitation with 2 μg lamin B1 antibody or without antibody (beads alone, used as negative control). Protein G-agarose beads (Sigma-Aldrich) were added to samples, and the mixtures were incubated for 4 h at 4°C under rotary agitation. After four washes, immunoprecipitates were resuspended in 2 × Laemmli buffer and boiled for 5 min. Following centrifugation, the supernatant was separated by 8% SDS–PAGE, and lamin B1 and p-p38 MAPK were detected by autoradiography.

In-vitro phosphorylation of immunoprecipitated lamin B1 by activated p38 MAPK

The kinase activity of p38 MAPK was estimated by measuring the phosphorylation rate of immunoprecipitated lamin B1. The SV40 fibroblasts were lysed for 30 min on ice in an RIPA (50 mM Tris HCl pH 8, 150 mM NaCl, 1% NP-40, 0.5% sodium deoxycholate and 0.1% SDS) buffer containing phosphatases and protease inhibitors. To improve the efficiently of extraction, we repeated mechanical disruption by passing the lysate 10 times through a needle attached to a 0.3-ml syringe. After centrifugation at 13 000 *g* for 30 min at 4°C, lysates were precleared and incubated (250 μg proteins) overnight at 4°C with 2 μg lamin B1 under agitation. Protein G-agarose beads (Sigma-Aldrich) were added to samples, and the mixtures were incubated for 4 h at 4°C under rotary agitation. After four washes, immunoprecipitates of lamin B1 or 2 μg of ATF-2 fusion protein (a p38 MAPK substrate, used as positive control) were resuspended in 30 μl kinase buffer containing 1 μg of recombinant α-p38 MAPK, 1 μg of recombinant MKK3 (Cell Signaling Technology Inc.), 5 μM ATP and 5 μCi [γ-^{32}P]ATP. After incubation for 15 min at 30°C, reactions were stopped on ice by the addition of 2 × Laemmli buffer. Samples were separated by 10% SDS–PAGE, and phosphorylated ^{32}P-lamin B1 was detected by autoradiography.

Statistical analysis

The results are expressed as the means ± s.e.m. of at least three independent experiments. Statistical analyses were performed using the non-parametric Mann–Whitney *t*-test, and * represents statistical significance ($P \leqslant 0.05$). For lamin B1 fluorescence intensity, the mean of circularity and PLA quantification, statistical analyses were performed using the non-parametric *T*-test, and *** represents statistical significance ($P \leqslant 0.0001$).

Supplementary data

Supplementary data are available at *The EMBO Journal* Online (http://www.embojournal.org).

Acknowledgements

We would like to thank Caroline Chabance for efficient technical assistance; Sophie Zinn-Justin, Carl Mann, J-Y Thuret (iBiTec, CEA,

DSV, Saclay), Filippo Rosselli, Corine Dupuy (IGR, Villejuif) and the members of the laboratory for helpful discussions; François Chevalier (Proteomic facility of IRCM) for technical advice and Thierry Kortulewski (microscopy facility, IRCM) for developing a specific program on CellProfiler. We thank Dr Narita (Cambridge, UK) for providing the ER-activated Ras-expressing cell line. AB and NI were supported by a CEA DSV fellowship. DG is a recipient of the CEA DSV IRTELIS international PhD fellowship. This work was supported by the Association pour la Recherche contre Cancer, Ligue Nationale Contre le Cancer (Ile de France comitee) and DSV-CEA 'Radiobiology grant.' BSL is sponsored by the Institut National du Cancer (INCa).

Author contributions: PB and BSL conceived the project and experiments; AB conceived and performed most of the experiments; CLC performed most of the oncogene-induced senescence (OIS) and IR-induced senescence experiments; DG performed some OIS and WB experiments; GP performed PLA experiments, some SA-β-gal assays; NI performed preliminary proteomic analysis; PB and BSL wrote the manuscript.

Conflict of interest

The authors declare that they have no conflict of interest.

References

Bartek J, Bartkova J, Lukas J (2007) DNA damage signalling guards against activated oncogenes and tumour progression. *Oncogene* **26:** 7773–7779

Bartkova J, Rezaei N, Liontos M, Karakaidos P, Kletsas D, Issaeva N, Vassiliou LV, Kolettas E, Niforou K, Zoumpourlis VC, Takaoka M, Nakagawa H, Tort F, Fugger K, Johansson F, Sehested M, Andersen CL, Dyrskjot L, Orntoft T, Lukas J *et al* (2006) Oncogene-induced senescence is part of the tumorigenesis barrier imposed by DNA damage checkpoints. *Nature* **444:** 633–637

Barzilai A, Biton S, Shiloh Y (2008) The role of the DNA damage response in neuronal development, organization and maintenance. *DNA Repair (Amst)* **7:** 1010–1027

Barzilai A, Rotman G, Shiloh Y (2002) ATM deficiency and oxidative stress: a new dimension of defective response to DNA damage. *DNA Repair (Amst)* **1:** 3–25

Biton S, Barzilai A, Shiloh Y (2008) The neurological phenotype of ataxia-telangiectasia: solving a persistent puzzle. *DNA Repair (Amst)* **7:** 1028–1038

Broers JL, Ramaekers FC, Bonne G, Yaou RB, Hutchison CJ (2006) Nuclear lamins: laminopathies and their role in premature ageing. *Physiol Rev* **86:** 967–1008

Browne SE, Roberts LJn, Dennery PA, Doctrow SR, Beal MF, Barlow C, Levine RL (2004) Treatment with a catalytic antioxidant corrects the neurobehavioral defect in ataxia-telangiectasia mice. *Free Radic Biol Med* **36:** 938–942

Campisi J, Andersen JK, Kapahi P, Melov S (2011) Cellular senescence: a link between cancer and age-related degenerative disease? *Semin Cancer Biol* **21:** 354–359

Cann KL, Hicks GG (2007) Regulation of the cellular DNA double-strand break response. *Biochem Cell Biol* **85:** 663–674

Cao K, Capell BC, Erdos MR, Djabali K, Collins FS (2007) A lamin A protein isoform overexpressed in Hutchinson-Gilford progeria syndrome interferes with mitosis in progeria and normal cells. *Proc Natl Acad Sci USA* **104:** 4949–4954

Coffinier C, Jung HJ, Nobumori C, Chang S, Tu Y, Barnes II RH, Yoshinaga Y, de Jong PJ, Vergnes L, Reue K, Fong LG, Young SG (2011) Deficiencies in lamin B1 and lamin B2 cause neurodevelopmental defects and distinct nuclear shape abnormalities in neurons. *Mol Biol Cell* **22:** 4683–4693

Collado M, Serrano M (2010) Senescence in tumours: evidence from mice and humans. *Nat Rev Cancer* **10:** 51–57

Cosentino C, Grieco D, Costanzo V (2011) ATM activates the pentose phosphate pathway promoting anti-oxidant defence and DNA repair. *EMBO J* **30:** 546–555

Debacq-Chainiaux F, Boilan E, Dedessus Le Moutier J, Weemaels G, Toussaint O (2010) p38(MAPK) in the senescence of human and murine fibroblasts. *Adv Exp Med Biol* **694:** 126–137

Dechat T, Adam SA, Taimen P, Shimi T, Goldman RD (2010) Nuclear lamins. *Cold Spring Harb Perspect Biol* **2:** a000547

di Masi A, D'Apice MR, Ricordy R, Tanzarella C, Novelli G (2008) The R527H mutation in LMNA gene causes an increased sensitivity to ionizing radiation. *Cell Cycle* **7:** 2030–2037

Di Micco R, Fumagalli M, Cicalese A, Piccinin S, Gasparini P, Luise C, Schurra C, Garre' M, Nuciforo PG, Bensimon A, Maestro R, Pelicci PG, d'Adda di Fagagna F (2006) Oncogene-induced senescence is a DNA damage response triggered by DNA hyper-replication. *Nature* **444:** 638–642

Dimri GP, Lee X, Basile G, Acosta M, Scott G, Roskelley C, Medrano EE, Linskens M, Rubelj I, Pereira-Smith O, Peacoke M, Campisi J (1995) A biomarker that identifies senescent human cells in culture and in aging skin *in vivo*. *Proc Natl Acad Sci USA* **92:** 9363–9367

Ding SL, Shen CY (2008) Model of human aging: recent findings on Werner's and Hutchinson-Gilford progeria syndromes. *Clin Interv Aging* **3:** 431–444

Efeyan A, Murga M, Martinez-Pastor B, Ortega-Molina A, Soria R, Collado M, Fernandez-Capetillo O, Serrano M (2009) Limited role of murine ATM in oncogene-induced senescence and p53-dependent tumor suppression. *PLoS One* **4:** e5475

Fredriksson S, Gullberg M, Jarvius J, Olsson C, Pietras K, Gustafsdottir SM, Ostman A, Landegren U (2002) Protein detection using proximity-dependent DNA ligation assays. *Nat Biotechnol* **20:** 473–477

Freund A, Patil CK, Campisi J (2011) p38MAPK is a novel DNA damage response-independent regulator of the senescence-associated secretory phenotype. *EMBO J* **30:** 1536–1548

Gil Del Valle L (2010) Oxidative stress in aging: theoretical outcomes and clinical evidences in humans. *Biomed Pharmacother* (doi:10.1016/j.biopha.2010.09.010)

Goldman RD, Gruenbaum Y, Moir RD, Shumaker DK, Spann TP (2002) Nuclear lamins: building blocks of nuclear architecture. *Genes Dev* **16:** 533–547

Gonzalez-Suarez I, Redwood AB, Gonzalo S (2009a) Loss of A-type lamins and genomic instability. *Cell Cycle* **8:** 3860–3865

Gonzalez-Suarez I, Redwood AB, Perkins SM, Vermolen B, Lichtensztejin D, Grotsky DA, Morgado-Palacin L, Gapud EJ, Sleckman BP, Sullivan T, Sage J, Stewart CL, Mai S, Gonzalo S (2009b) Novel roles for A-type lamins in telomere biology and the DNA damage response pathway. *EMBO J* **28:** 2414–2427

Gruenbaum Y, Margalit A, Goldman RD, Shumaker DK, Wilson KL (2005) The nuclear lamina comes of age. *Nat Rev Mol Cell Biol* **6:** 21–31

Guo Z, Kozlov S, Lavin MF, Person MD, Paull TT (2010) ATM activation by oxidative stress. *Science* **330:** 517–521

Haithcock E, Dayani Y, Neufeld E, Zahand AJ, Feinstein N, Mattout A, Gruenbaum Y, Liu J (2005) Age-related changes of nuclear architecture in Caenorhabditis elegans. *Proc Natl Acad Sci USA* **102:** 16690–16695

Han J, Sun P (2007) The pathways to tumor suppression via route p38. *Trends Biochem Sci* **32:** 364–371

Harman D (1956) Aging: a theory based on free radical and radiation chemistry. *J Gerontol* **11:** 298–300

Ito K, Hirao A, Arai F, Takubo K, Matsuoka S, Miyamoto K, QJ;Ohmura M, Naka K, Hosokawa K, Ikeda Y, Suda T (2006) Reactive oxygen species act through p38 MAPK to limit the lifespan of hematopoietic stem cells. *Nat Med* **12:** 446–451

Ito K, Takubo K, Arai F, Satoh H, Matsuoka S, Ohmura M, Naka K, Azuma M, Miyamoto K, Hosokawa K, Ikeda Y, Mak TW, Suda T, Hirao A (2007) Regulation of reactive oxygen species by Atm is essential for proper response to DNA double-strand breaks in lymphocytes. *J Immunol* **178:** 103–110

Iwasa H, Han J, Ishikawa F (2003) Mitogen-activated protein kinase p38 defines the common senescence-signalling pathway. *Genes Cells* **8:** 131–144

Kudlow BA, Kennedy BK, Monnat RJJ (2007) Werner and Hutchinson-Gilford progeria syndromes: mechanistic basis of human progeroid diseases. *Nat Rev Mol Cell Biol* **8:** 394–404

Lammerding J, Fong LG, Ji JY, Reue K, Stewart CL, Young SG, Lee RT (2006) Lamins A and C but not lamin B1 regulate nuclear mechanics. *J Biol Chem* **281:** 25768–25780

Lans H, Hoeijmakers JH (2006) Cell biology: ageing nucleus gets out of shape. *Nature* **440:** 32–34

Laulier C, Barascu A, Guirouilh-Barbat J, Pennarun G, Le Chalony C, Chevalier F, Palierne G, Bertrand P, Verbavatz JM, Lopez BS (2011) Bcl-2 inhibits nuclear homologous recombination by localizing BRCA1 to the endomembranes. *Cancer Res* **71:** 3590–3602

Lavin MF (2008) Ataxia-telangiectasia: from a rare disorder to a paradigm for cell signalling and cancer. *Nat Rev Mol Cell Biol* **9:** 759–769

Lavin MF, Gueven N, Bottle S, Gatti RA (2007) Current and potential therapeutic strategies for the treatment of ataxia-telangiectasia. *Br Med Bull* **81–82:** 129–147

Lavin MF, Kozlov S (2007) ATM activation and DNA damage response. *Cell Cycle* **6:** 931–942

Lee AC, Fenster BE, Ito H, Takeda K, Bae NS, Hirai T, Yu ZX, Ferrans VJ, Howard BH, Finkel T (1999) Ras proteins induce senescence by altering the intracellular levels of reactive oxygen species. *J Biol Chem* **274:** 7936–7940

Li B, Jog S, Candelario J, Reddy S, Comai L (2009) Altered nuclear functions in progeroid syndromes: a paradigm for aging research. *ScientificWorldJournal* **9:** 1449–1462

Lin ST, Fu YH (2009) miR-23 regulation of lamin B1 is crucial for oligodendrocyte development and myelination. *Dis Model Mech* **2:** 178–188

Liu B, Wang J, Chan KM, Tjia WM, Deng W, Guan X, Huang JD, Li KM, Chau PY, Chen DJ, Pei D, Pendas AM, Cadinanos J, Lopez-Otin C, Tse HF, Hutchison C, Chen J, Cao Y, Cheah KS, Tryggvason K *et al* (2005) Genomic instability in laminopathy-based premature aging. *Nat Med* **11:** 780–785

Liu B, Zhou Z (2008) Lamin A/C, laminopathies and premature ageing. *Histol Histopathol* **23:** 747–763

Liu Y, Rusinol A, Sinensky M, Wang Y, Zou Y (2006) DNA damage responses in progeroid syndromes arise from defective maturation of prelamin A. *J Cell Sci* **119:** 4644–4649

Lu T, Finkel T (2008) Free radicals and senescence. *Exp Cell Res* **314:** 1918–1922

Malhas AN, Lee CF, Vaux DJ (2009) Lamin B1 controls oxidative stress responses via Oct-1. *J Cell Biol* **184:** 45–55

Malhas AN, Vaux DJ (2009) Transcription factor sequestration by nuclear envelope components. *Cell Cycle* **8:** 959–960

Manju K, Muralikrishna B, Parnaik VK (2006) Expression of disease-causing lamin A mutants impairs the formation of DNA repair foci. *J Cell Sci* **119:** 2704–2714

Matsuoka S, Ballif BA, Smogorzewska A, McDonald ERr, Hurov KE, Luo J, Bakalarski CE, Zhao Z, Solimini N, Lerenthal Y, Shiloh Y, Gygi SP, Elledge SJ (2007) ATM and ATR substrate analysis reveals extensive protein networks responsive to DNA damage. *Science* **316:** 1160–1166

Matsuzawa A, Ichijo H (2008) Redox control of cell fate by MAP kinase: physiological roles of ASK1-MAP kinase pathway in stress signaling. *Biochim Biophys Acta* **1780:** 1325–1336

McClintock D, Ratner D, Lokuge M, Owens DM, Gordon LB, Collins FS, Djabali K (2007) The mutant form of lamin A that causes Hutchinson-Gilford progeria is a biomarker of cellular aging in human skin. *PLoS One* **2:** e1269

Meijer IA, Simoes-Lopes AA, Laurent S, Katz T, St-Onge J, Verlaan DJ, Dupre N, Thibault M, Mathurin J, Bouchard JP, Rouleau GA (2008) A novel duplication confirms the involvement of 5q23.2 in autosomal dominant leukodystrophy. *Arch Neurol* **65:** 1496–1501

Misteli T, Scaffidi P (2005) Genome instability in progeria: when repair gets old. *Nat Med* **11:** 718–719

Muller FL, Lustgarten MS, Jang Y, Richardson A, Van Remmen H (2007) Trends in oxidative aging theories. *Free Radic Biol Med* **43:** 477–503

Naka K, Tachibana A, Ikeda K, Motoyama N (2004) Stress-induced premature senescence in hTERT-expressing ataxia telangiectasia fibroblasts. *J Biol Chem* **279:** 2030–2037

Padiath QS, Saigoh K, Schiffmann R, Asahara H, Yamada T, Koeppen A, Hogan K, Ptacek LJ, Fu YH (2006) Lamin B1 duplications cause autosomal dominant leukodystrophy. *Nat Genet* **38:** 1114–1123

Pan JS, Hong MZ, Ren JL (2009) Reactive oxygen species: a double-edged sword in oncogenesis. *World J Gastroenterol* **15:** 1702–1707

Parnaik VK, Manju K (2006) Laminopathies: multiple disorders arising from defects in nuclear architecture. *J Biosci* **31:** 405–421

Prokocimer M, Davidovich M, Nissim-Rafinia M, Wiesel-Motiuk N, Bar DZ, Barkan R, Meshorer E, Gruenbaum Y (2009) Nuclear lamins: key regulators of nuclear structure and activities. *J Cell Mol Med* **13:** 1059–1085

Redwood AB, Perkins SM, Vanderwaal RP, Feng Z, Biehl KJ, Gonzalez-Suarez I, Morgado-Palacin L, Shi W, Sage J, Roti-Roti JL, Stewart CL, Zhang J, Gonzalo S (2011) A dual role for A-type lamins in DNA double-strand break repair. *Cell Cycle* **10:** 2549–2560

Reliene R, Fleming SM, Chesselet MF, Schiestl RH (2008) Effects of antioxidants on cancer prevention and neuromotor performance in Atm deficient mice. *Food Chem Toxicol* **46:** 1371–1377

Reliene R, Schiestl RH (2006) Antioxidant N-acetyl cysteine reduces incidence and multiplicity of lymphoma in Atm deficient mice. *DNA Repair (Amst)* **5:** 852–859

Reliene R, Schiestl RH (2007) Antioxidants suppress lymphoma and increase longevity in Atm-deficient mice. *J Nutr* **137:** 229S–232S

Rodier F, Campisi J (2011) Four faces of cellular senescence. *J Cell Biol* **192:** 547–556

Rodier F, Coppe JP, Patil CK, Hoeijmakers WA, Munoz DP, Raza SR, Freund A, Campeau E, Davalos AR, Campisi J (2009) Persistent DNA damage signalling triggers senescence-associated inflammatory cytokine secretion. *Nat Cell Biol* **11:** 973–979

Rodriguez S, Coppede F, Sagelius H, Eriksson M (2009) Increased expression of the Hutchinson-Gilford progeria syndrome truncated lamin A transcript during cell aging. *Eur J Hum Genet* **17:** 928–937

Rotman G, Shiloh Y (1999) ATM: a mediator of multiple responses to genotoxic stress. *Oncogene* **18:** 6135–6644

Scaffidi P, Misteli T (2006) Lamin A-dependent nuclear defects in human aging. *Science* **312:** 1059–1063

Schubert R, Erker L, Barlow C, Yakushiji H, Larson D, Russo A, Mitchell JB, Wynshaw-Boris A (2004) Cancer chemoprevention by the antioxidant tempol in Atm-deficient mice. *Hum Mol Genet* **13:** 1793–1802

Shiloh Y (2006) The ATM-mediated DNA-damage response: taking shape. *Trends Biochem Sci* **31:** 402–410

Soderberg O, Gullberg M, Jarvius M, Ridderstrale K, Leuchowius KJ, Jarvius J, Wester K, Hydbring P, Bahram F, Larsson LG, Landegren U (2006) Direct observation of individual endogenous protein complexes *in situ* by proximity ligation. *Nat Methods* **3:** 995–1000

Soderberg O, Leuchowius KJ, Gullberg M, Jarvius M, Weibrecht I, Larsson LG, Landegren U (2008) Characterizing proteins and their interactions in cells and tissues using the *in situ* proximity ligation assay. *Methods* **45:** 227–232

Tantin D, Schild-Poulter C, Wang V, Hache RJ, Sharp PA (2005) The octamer binding transcription factor Oct-1 is a stress sensor. *Cancer Res* **65:** 10750–10758

Thornton TM, Rincon M (2009) Non-classical p38 map kinase functions: cell cycle checkpoints and survival. *Int J Biol Sci* **5:** 44–51

Torres M, Forman HJ (2003) Redox signaling and the MAP kinase pathways. *Biofactors* **17:** 287–296

Vergnes L, Péterfy M, Bergo MO, Young SG, Reue K (2004) Lamin B1 is required for mouse development and nuclear integrity. *Proc Natl Acad Sci USA* **101:** 10428–10433

Wang W, Chen JX, Liao R, Deng Q, Zhou JJ, Huang S, Sun P (2002) Sequential activation of the MEK-extracellular signal-regulated kinase and MKK3/6-p38 mitogen-activated protein kinase pathways mediates oncogenic ras-induced premature senescence. *Mol Cell Biol* **22:** 3389–3403

Worman HJ, Bonne G (2007) 'Laminopathies': a wide spectrum of human diseases. *Exp Cell Res* **313:** 2121–2133

